



Development of Industrial Servo Control System for Elevator-Door Mechanism Actuated by Direct-Drive Induction Machine

Rong-Jong Wai and Jeng-Dao Lee

*Department of Electrical Engineering, Yuan Ze University,
Chung Li 32026, Taiwan, R.O.C.*

Received: April 25, 2003; Revised: March 26, 2004

Abstract: In this study, an industrial sliding-mode servo control system is developed for the motion control of a direct-drive-type elevator-door servomechanism. The mechanical structure and dynamic analyses of an elevator-door mechanism with an indirect field-oriented induction servomotor drive is described initially. Moreover, a newly designed total sliding-mode control (TSMC) system, which is insensitive to uncertainties in the whole control process, is introduced. In addition, numerical simulation and experimental results due to specific position and velocity profiles are provided to verify the effectiveness of the proposed control scheme with regard to parameter variations and external disturbance. Furthermore, the merits of the TSMC system are exhibited in comparison with computed torque control (CTC) and conventional sliding-mode control (CSMC). The salient features of this study are 1) the controlled system has a total sliding motion without a reaching phase and no chattering torque, and 2) this simple control strategy is easily implemented by hardware/software to an industrial servo controller.

Keywords: *Sliding-mode control; computed torque control; indirect field-oriented; induction servomotor drive; elevator door.*

Mathematics Subject Classification (2000): 70B15, 68T40, 93C85.

1 Introduction

Most nonlinear mechanism systems comprise driven motors, coupling gears and the nonlinear mechanism. Therefore, complex modeling procedures are usually required to design a suitable control scheme. Besides, there are many uncertainties such as system parameter variations, external disturbance, friction force and unmodelled dynamics to influence

the prior-designed control characteristics in industrial applications. Though many modern control techniques have been designed to control the nonlinear mechanism systems by using complex control laws with high control efforts, degraded control performances are often resulted due to the existence of uncertainty [1]. Thus it is natural to explore other nonlinear controls that can circumvent the problem of uncertainties and achieve better compensation and global stability [2]–[4].

Sliding-mode control (SMC) has been demonstrated to be an effective nonlinear robust control approach for controlling electric drive systems since it provides system dynamics with an invariance property to uncertainties once the system dynamics are controlled in the sliding mode [2]–[3]. It offers a fast dynamic response, a stable control system and an easy hardware/software implementation. However, this control strategy produces some drawbacks associated with the large torque chattering that may excite mechanical resonance and unstable dynamics. Besides, the insensitivity of the controlled system to uncertainties only exists in the sliding mode, but not during the reaching phase. Thus the system dynamic in the reaching phase is still influenced by uncertainties. To keep robustness in the whole sliding-mode control system, several researchers have focused on eliminating the effect of the reaching phase [5]–[8]. A newly-designed sliding curve, that is chosen as close as possible to time-optimal trajectory, was proposed in Harashima, *et al.* [5] and Hashimoto, *et al.* [6] to keep robustness from the initial point to final point. Gao and Hung [7] partially shaped the reaching law to specify the system dynamics in the reaching phase. However, the system dynamics are still subjected to uncertainties. Therefore, this study adopts the idea of total sliding-mode control [8] to get a sliding motion through the entire state trajectory. In other words, no reaching phase exists in the control process. Thus the controlled system during the whole control process is insensitive to the occurrence of uncertainties.

In the past several decades, dc motors have been widely used in factory automation as high-performance drives. However, the mechanical commutators and brush assembly make dc motors much more expensive than ac motors. Besides, the use of mechanical commutators may produce undesired sparks that are not allowed in some applications. As compared with dc motor, an induction motor (IM) is robust, cheap and easily maintained. These characteristics make it desirable to employ them in variable-speed or servo system. However, its control characteristics are more complicated than the dc motors. In the scalar control techniques, the transient dipping of flux reduces the torque sensitivity with slip and lengthens the response time. In order to overcome the foregoing limitation, the field-oriented control technique has been widely used in industry for high-performance IM drive [9]–[10]. With the field-oriented control approach, the dynamic behavior of an IM is rather similar to that of a separately excited dc motor. Thus, the IM has been adopted widely as a driver in the elevator system recently [11]. However, a traditional open-loop scalar (constant V/f ratio) controller with a gear transmission is always utilized in the control of elevator car or automatic door. The motivation of this study is to develop a total sliding-mode servo controller for a gearless elevator-door mechanism actuated with direct-drive-type IM [12]–[13].

2 Mechanical Structure and Dynamic Analyses

The mechanical structure and drive system of an elevator-door servomechanism is depicted in Figure 2.1, which is composed of a direct-drive-type induction servomotor, single-side-opened elevator door, belting and weighting mechanisms. In Figure 2.1, the

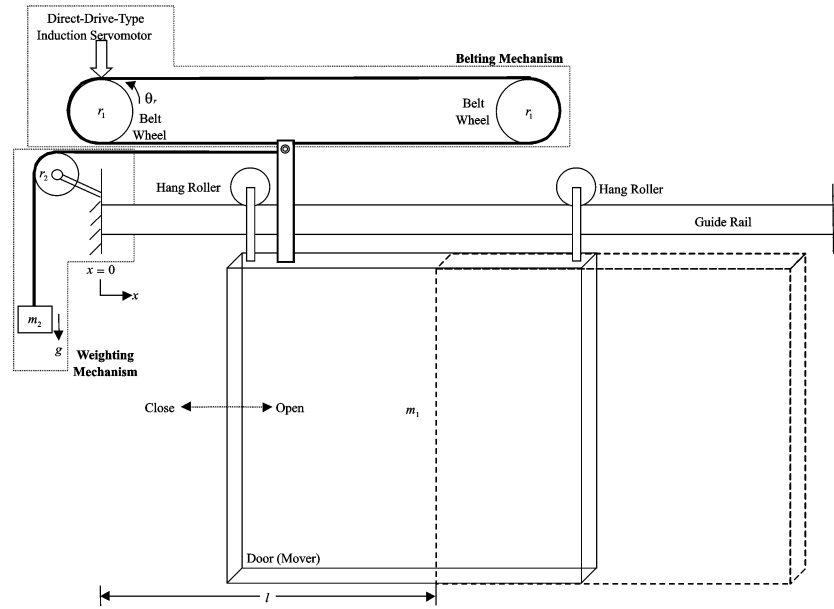


Figure 2.1. Mechanical structure and drive system of elevator-door servomechanism.

symbols m_1 and m_2 represent the masses of door and counterweight, respectively; r_1 and r_2 denote the radiuses of belting and weighting wheels, respectively; θ_r is the rotor position of the induction servomotor; x is the moving position of the door, l is the total length of the moving path, and g is the gravity acceleration.

A Direct-Drive-Type Induction Servomotor

The vocabulary “direct-drive” means that the transmittal mechanism is passed through belts directly without a gearbox. The configuration of an indirect field-oriented induction servomotor drive system is depicted in Figure 2.2(a) [8]. It consists of an induction servomotor coupled with a mechanism, a ramp comparison current-controlled pulse-width-modulation (PWM) voltage source inverter (VSI), a unit vector generator (where θ_e is the position of rotor flux), a coordinate translator, a speed control loop and a position control loop. The induction servomotor used in this drive system is a three-phase Y-connected eight-pole 150W 60Hz 220V/3.3A type. The current-controlled VSI is implemented by insulated gate bipolar transistor (IGBT) switching components with a switching frequency of 15kHz. The mechanical equation of an induction servomotor drive can be represented as

$$J\ddot{\theta}_r(t) + B\dot{\theta}_r(t) + T_L = T_e, \quad (1)$$

where J is the moment of inertia; B is the damping coefficient; T_L represents the load torque and external disturbance; T_e denotes the electric torque. With the implementation of field-oriented control [9]–[10], the induction servomotor drive system can be simplified to a control system block diagram as shown in Figure 2.2(b), in which the electric torque can be represented as

$$T_e = K_t i_{qs}^* \quad (2)$$

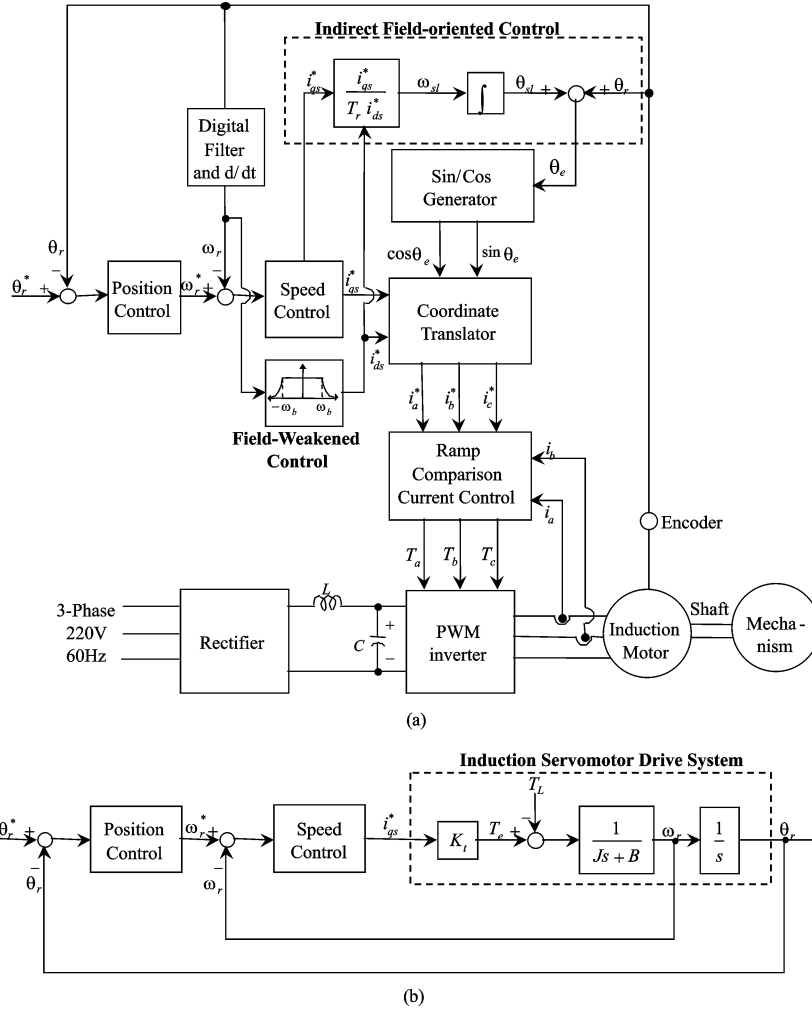


Figure 2.2. (a) Indirect field-oriented induction servomotor drive. (b) Simplified control system.

with

$$K_t = \frac{3n_p}{2} \frac{L_m^2}{L_r} i_{ds}^*, \quad (3)$$

where K_t is the torque constant; i_{qs}^* is the torque current command; i_{ds}^* is the flux current command; n_p is the number of pole pairs; L_m is the magnetizing inductance per phase; L_r is the rotor inductance per phase; ω_r is the rotor speed; θ_r^* and ω_r^* are the rotor position and speed commands.

B Dynamic Model of Elevator-Door Servomechanism

The Newtonian motion law is utilized to derive the dynamic equation of the elevator-door servomechanism in this subsection. Since the belt makes the electric torque convert into the linear driving force and the control object is the door position, the conversion

relationship between the rotor position and door position is

$$\theta_r(t) = x(t)/r_1. \quad (4)$$

Substituting (4) into (1) and using (2), one can obtain

$$J\ddot{x}(t) + B\dot{x}(t) = r_1 K_t i_{qs}^* - r_1 T_L. \quad (5)$$

Consider (5), the in the elevator-door servomechanism is

$$T_L = T_i + T_w + T_f + T_d, \quad (6)$$

where $T_i = (m_1 + m_2)r_1\ddot{x}$ represents the load inertia torque; $T_w = m_2gr_1\text{sgn}(\dot{x})$ denotes the weighting torque, in which $\text{sgn}(\cdot)$ is a sign function; $T_f = \mu m_1 g$ exhibits the friction torque between the hang roller and guide rail, in which μ is the friction coefficient; T_d is the external disturbance torque. Combined (5) with (6), the complete dynamic equation of the elevator-door servomechanism can be obtained as

$$\ddot{x}(t) \equiv A_p \dot{x}(t) + B_p U(t) + C_p + D_p, \quad (7)$$

where $U(t) = i_{qs}^*(t)$ is the control input, and

$$\begin{aligned} A_p &= -B[J + r_1^2(m_1 + m_2)]^{-1}, \\ B_p &= r_1 K_t [J + r_1^2(m_1 + m_2)]^{-1} > 0, \\ C_p &= -[J + r_1^2(m_1 + m_2)]^{-1} [r_1 m_2 \text{sgn}(\dot{x}) + \mu m_1] r_1 g, \\ D_p &= -r_1 [J + r_1^2(m_1 + m_2)]^{-1} T_d, \end{aligned}$$

Note that, the unmodelled dynamics, e.g. the friction existing in the belting mechanism, can be considered as the external disturbance torque. The most important parameters that affect the control performance of the elevator-door servomechanism are the external disturbance torque T_d and the variations of motor parameters.

3 Total Sliding-Mode Control

Consider the system parameters in nominal conditions without external disturbance torque, rewriting (7) as follows can represent the nominal model of the elevator-door servomechanism:

$$\ddot{x}(t) = A_{pn} \dot{x}(t) + B_{pn} U(t) + C_{pn}, \quad (8)$$

where A_{pn} , B_{pn} and C_{pn} are the nominal values of A_p , B_p and C_p , respectively. Consider (8) parametric variation, external disturbance and unpredictable uncertainties for the actual elevator-door servomechanism

$$\begin{aligned} \ddot{x}(t) &= (A_{pn} + \Delta A) \dot{x}(t) + (B_{pn} + \Delta B) U(t) + (C_{pn} + \Delta C) + D_p + \beta \\ &\equiv A_{pn} \dot{x}(t) + B_{pn} U(t) + C_{pn} + W(t), \end{aligned} \quad (9)$$

where ΔA , ΔB and ΔC denote the uncertainties introduced by the variations of motor parameters; β represents the unstructured uncertainty due to nonideal field orientation in

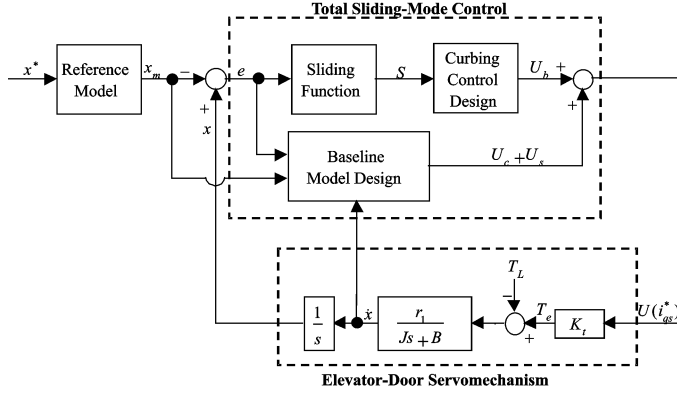


Figure 3.1. Block diagram of TSMC system.

transient state, and the unpredictable dynamics in practical applications; $W(t)$ is called the lumped uncertainty and is defined as

$$W(t) = \Delta A \dot{x}(t) + \Delta B U(t) + \Delta C + D_p + \beta. \quad (10)$$

Here the bound of the lumped uncertainty is assumed to be given; that is,

$$|W(t)| < \rho, \quad (11)$$

where ρ is a given positive constant. The control problem is to find a control law so that the state χ can track specific desired trajectories in the presence of uncertainties. To achieve this control objective, define the tracking error $e = x - x_m$, in which x_m represents a desired position specified by a reference model. The presentation of TSMC for the elevator-door servomechanism is divided into two main parts and is depicted in Figure 3.1. The first part addresses performance design. The object is to specify the desired performance in terms of the nominal model, and it is referred to as baseline model design. Following the baseline model design, the second part is the curbing controller design to totally eliminate the unpredictable perturbation effect from the parameter variations and external disturbance so that the baseline model design performance can be exactly assured. Define a sliding function $S(t)$ as follows [8]:

$$S(t) = C(\mathbf{E}) - C(\mathbf{E}_0) - \int_0^t \frac{\partial C}{\partial \mathbf{E}^T} \mathbf{A} \mathbf{E} d\tau, \quad (12)$$

where $C(\mathbf{E})$ is a scalar variable designed as $\frac{\partial C}{\partial \mathbf{E}^T} = [0 \ B_{pn}^{-1}]$; \mathbf{E}_0 is the initial state of $\mathbf{E}(t)$, and

$$\mathbf{E} = [e \ \dot{e}]^T \quad \mathbf{A} = \begin{pmatrix} 0 & 1 \\ -K_p & -K_v \end{pmatrix} \quad (13)$$

in which K_p and K_v are positive constants. Note that, since the function $S(t) = 0$ when $t = 0$, there is no reaching phase as in the traditional sliding-mode control [2]–[3]. Then, the TSMC law is assumed to take the following form:

$$U(t) = U_c(t) + U_s(t) + U_b(t) \quad (14)$$

with

$$U_c(t) = -B_{pn}^{-1}[A_{pn}\dot{x}(t) + C_{pn}], \quad (15)$$

$$U_s(t) = B_{pn}^{-1}[\ddot{\chi}(t) - K_p e(t) - K_v \dot{e}(t)], \quad (16)$$

$$U_b(t) = -KS(t) - \rho B_{pn}^{-1} \text{sgn}(S(t)), \quad (17)$$

where K is a positive constant. The first controller, U_c , is used to compensate for the nonlinear effects and attempts to cancel the nonlinear terms in the model. After the nonlinear model is linearized, the second controller, U_s , is used to specify the desired system performance. The objective of the third controller U_b is to keep the controlled system dynamics on the surface $S(t) = 0$. That is, curb the system dynamics onto $S(t) = 0$ for all time. Thus U_b is called a curbing controller, which is a constant plus proportional rate control scheme providing a measure for the reduction of chattering [14].

Substitute (14), (15) and (16) into (9), the state variable form can be obtained as follows:

$$\dot{\mathbf{E}} = \mathbf{A}\mathbf{E} + \mathbf{B}_m[U_b(t) + B_{pn}^{-1}W(t)], \quad (18)$$

where $\mathbf{B}_m = [0 \ B_{pn}]^T$. Now $S(t) = 0$ when $t = 0$. To maintain the state on the surface $S(t) = 0$ for all time, one only needs to show that

$$S(t)\dot{S}(t) < 0, \quad \text{if } S(t) \neq 0. \quad (19)$$

Differentiating $S(t)$ shown in (12) with respect to time and using error dynamics shown in (19) yields

$$\begin{aligned} \dot{S}(t) &= \frac{\partial C}{\partial \mathbf{E}^T} \dot{\mathbf{E}} - \frac{\partial C}{\partial \mathbf{E}^T} \mathbf{A}\mathbf{E} = \frac{\partial C}{\partial \mathbf{E}^T} \{ \mathbf{A}\mathbf{E} + \mathbf{B}_m[U_b(t) + B_{pn}^{-1}W(t)] - \mathbf{A}\mathbf{E} \} \\ &= U_b(t) + B_{pn}^{-1}W(t). \end{aligned} \quad (20)$$

Multiplying $S(t)$ by (20) and inserting control U_b shown in (17) into (20) yields

$$\begin{aligned} S(t)\dot{S}(t) &= S(t)[U_b(t) + B_{pn}^{-1}W(t)] \leq S(t)U_b(t) + B_{pn}^{-1}|S(t)||W(t)| \\ &= -KS^2(t) - \rho B_{pn}^{-1}|S(t)| + B_{pn}^{-1}|S(t)||W(t)| < -KS^2(t) < 0. \end{aligned} \quad (21)$$

Thus the sliding mode can be assured throughout the whole control period. Wai [8] presented an adaptive sliding-mode control system to control the position of an induction servo motor drive, where a simple adaptive algorithm was utilized to estimate the bound of uncertainties in the curbing controller of total sliding-mode control system for reducing the chattering torque. However, the adaptation law for the bound of uncertainties is always positive and tracking error introduced by any uncertainty will cause the estimated bound growth. It implies that the curbing controller will result in large chattering with time gradually. This results that the IM will eventually be saturated and the system may be unstable. Wai [15] described the dynamic responses of a recurrent-fuzzy-neural-network (RFNN) sliding-mode controlled permanent magnet synchronous servomotor, where a RFNN bound observer was utilized to adjust the uncertainty bounds in the curbing controller of total sliding-mode control system. Although it can solve the problem of parameter divergence, this control scheme seems to be more complicate such that it is

difficult to implement in practical applications. Compared the modified control strategy used in this study with our previous works [8, 15], it can reduce effectively the chattering phenomena without any auxiliary algorithms such that this simple control scheme can be easily implemented in industrial applications. The effectiveness of the proposed TSMC system is verified by the following numerical simulation and experimental results.

4 Numerical Simulation and Experimental Results

For numerical simulations, the parameters of the elevator-door mechanism are designed as follows:

$$\begin{aligned} m_1 &= 20\text{kg}, & m_2 &= 1.5\text{kg}, & g &= 9.8, & \mu &= 0.1, \\ r_1 &= 1.417 \times 10^{-2}\text{m}, & r_2 &= 4.2 \times 10^{-2}\text{m}, & l &= 1.2\text{m}. \end{aligned} \quad (22)$$

Moreover, the parameters of the direct-drive-type induction servomotor system are

$$K_t = 0.4851\text{Nm/A}, \quad \bar{J} = 4.78 \times 10^{-3}\text{Nms}^2/\text{rad}, \quad \bar{B} = 5.34 \times 10^{-3}\text{Nms}/\text{rad}, \quad (23)$$

where the overbar symbol represents the system parameter in the nominal condition. In addition, the gains of the proposed TSMC control system are given as

$$K_\nu = 14, \quad K_p = 49, \quad \rho = 0.1, \quad K = 80. \quad (24)$$

Properly choosing the values of K_ν and K_p , the desired nominal system dynamics such as rise time, overshoot, and settling time can be easily designed by a second-order system, $\ddot{e} + K_\nu \dot{e} + K_p e = 0$. Moreover, the fixed bound ρ and the constant gain K in the curbing controller are determined roughly to achieve the superior transient control performance in both simulation and experimentation considering the requirement of stability and the possible operating conditions. Note that, introducing the constant gain K into the curbing controller can tune the convergent speed of the tracking performance and ensure the stability as the selection of a small value ρ for reducing the chattering phenomena induced by the sign function in the curbing controller. Two simulation cases including motor parameter variations and external disturbance torque in the mechanism are addressed as follows to verify the robust characteristic of the TSMC system: Case 1: $J = \bar{J}$, $B = \bar{B}$, $T_L = 1\text{Nm}$ occurring between 14s-16s; Case 2: $J = 3 \times \bar{J}$, $B = 3 \times \bar{B}$, $T_L = 1\text{Nm}$ occurring between 14s-16s. The control objective is to make the door position and velocity follow the specific reference profiles under the occurrence of uncertainties. The door position command is obtained based on the velocity profile of the elevator door. The door is moving from the left/right side to right/left side with $\pm 0.2\text{m/s}$ reference velocity.

In the simulation, firstly, the computed torque control (CTC) system that is equal to baseline model design ($U_c + U_s$) is demonstrated for comparison. The simulated results of CTC system at Case 1 and Case 2 are depicted in Figure 4.1. The position tracking are depicted in Figures 4.1(a) and 4.1(c), and the associated velocity response are depicted in Figures 4.1(b) and 4.1(d). From the simulated results, favorable tracking responses shown in the beginning of Figures 4.1(a) and 4.1(c) only can be obtained at the nominal condition, and poor tracking responses are resulted owing to the motor parameter variations and external disturbance torque. Though large control gains (K_ν and K_p) may solve the problem of delay or degenerate tracking responses, it will result

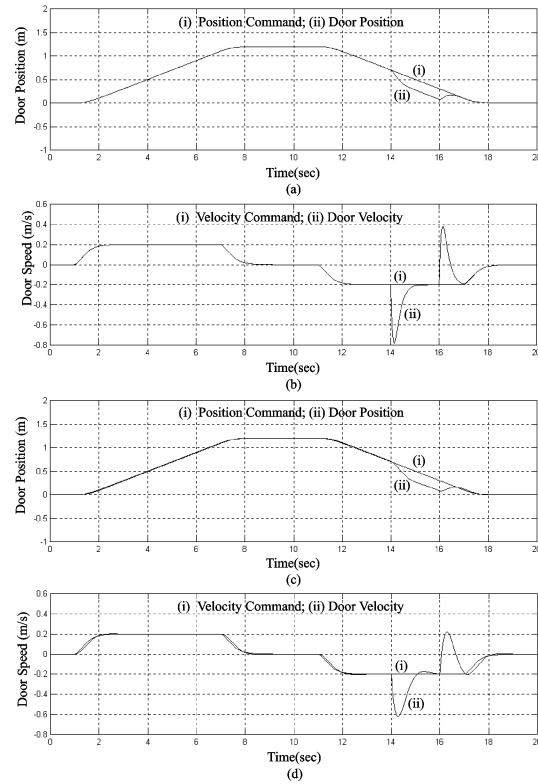


Figure 4.1. Simulated results of CTC system: (a) position tracking at Case 1; (b) velocity response at Case 1; (c) position tracking at Case 2; (d) velocity response at Case 2.

in impractical large control efforts. Therefore, the control gains are difficult to determine due to the unknown uncertainties in practical applications, and are ordinarily chosen as a compromise between the stability and control performance.

Secondly, the conventional sliding-model control (CSMC) designed by Slotine and Li [2] as follows is introduced to compare the control performance of the TSMC system:

$$U = U_{eq} + U_r \quad (25)$$

in which $U_{eq} = U_c + U_s$ is the equivalent control and $U_r = \alpha B_{pn}^{-1} \text{sgn}(S_L)$ is the hitting control, where $S_L = \dot{e} + \lambda e$; λ is a positive constant; α is the hitting gain that is selected to satisfy the sliding condition. The simulated results of CSMC system ($\lambda = 5$ and $\alpha = 8$) at Case 1 and Case 2 are depicted in Figure 4.2. The position tracking are depicted in Figures 4.2(a) and 4.2(c), and the associated velocity response are depicted in Figures 4.2(b) and 4.2(d). Compared Figure 4.2 with Figure 4.1, the CSMC system got the better control performance than the CTC system, especially under the occurrence of uncertainties. However, the chattering velocity responses show in Figures 4.2(b) and 4.2(d) are caused by the large selection of hitting-control gain, α . Although the chattering phenomena can be reduced with small hitting-control gain, it will result in degenerate control performance.

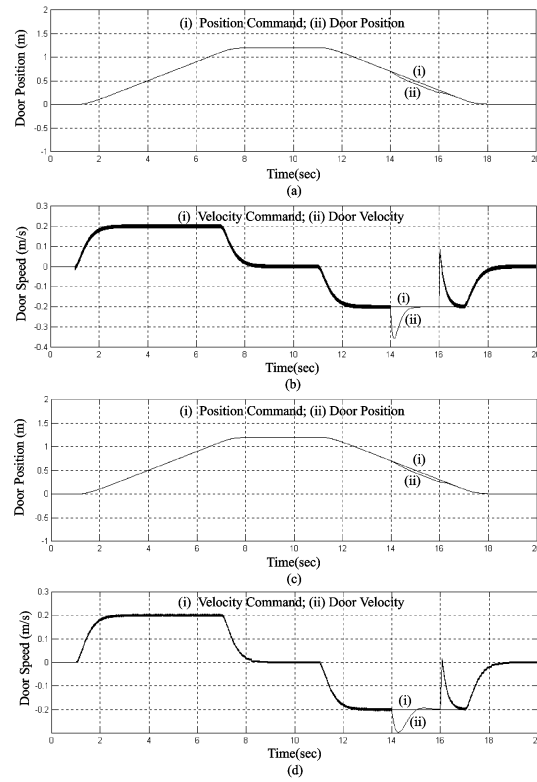


Figure 4.2. Simulated results of CSMC system: (a) position tracking at Case 1; (b) velocity response at Case 1; (c) position tracking at Case 2; (d) velocity response at Case 2.

Now, the designed TSMC system is simulated under the same cases, and its results are depicted in Figure 4.3. The chattering phenomenon does not exist in the velocity response of the TSMC system as shown in Figures 4.3(b) and 4.3(d). Moreover, the robust control performance of the TSMC system, both in the conditions of motor parameter variations and external disturbance torque, are obvious as shown in Figures 4.3(a) and 4.3(c). According to the above numerical simulation, the TSMC system yields the superior control performance than the CTC and CSMC systems.

The experimentation of the CTC, CSMC and TSMC systems for an actual elevator-door servomechanism are provided here to further demonstrate the advantage of the proposed TSMC control system. The PIC16F877 single chip micro-controller produced by Microchip company is used as a main CPU which has a 2ms control loop to implement the TSMC algorithm and a 0.2ms interrupt loop to execute current control inner loop with field-oriented mechanism. In the experimentation, a braking machine is driven by a current source drive to provide a disturbance torque, and an iron disk is coupled to the rotor shaft of an induction servomotor taking as an inertia varying mechanism.

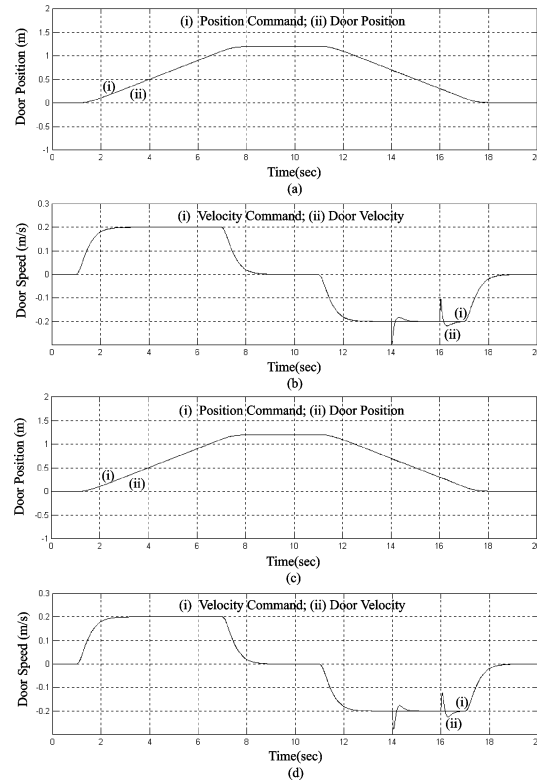


Figure 4.3. Simulated results of TSMC system: (a) position tracking at Case 1; (b) velocity response at Case 1; (c) position tracking at Case 2; (d) velocity response at Case 2.

Two experimental conditions are given to verify the robust control performance. One is the disturbance condition that is the nominal motor inertia with 1Nm disturbance torque occurring between 14s-16s. The other is the perturbed condition that is the increasing of the motor inertia to approximately three times the nominal value with 1Nm disturbance torque occurring between 14s-16s. The experimental results of CTC, CSMC and TSMC systems at disturbance and perturbed conditions are depicted in Figures 4.4 and 4.5, respectively. Note that, there are slight difference between the numerical simulation and experimental results due to the existence of unpredictable uncertainties in practical applications. It can be seen from the experimental results that the TSMC system tracks well with the specific position and velocity profiles during the whole operation. Consequently, the proposed TSMC system is more suitable to control the elevator-door servomechanism considering the existence of uncertainties.

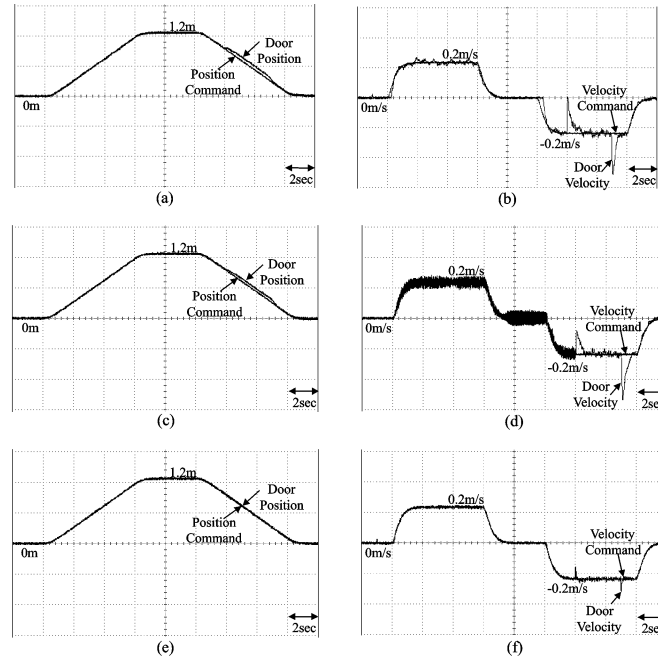


Figure 4.4. Experimental results of CTC, CSMC, TSMC systems at disturbance condition: (a) position tracking of CTC system; (b) velocity response of CTC system; (c) position tracking of CSMC system; (d) velocity response of CSMC system; (e) position tracking of TSMC system; (f) velocity response of TSMC system.

5 Conclusions

This study has successfully demonstrated the application of a total sliding-mode control system to control the motion of an elevator-door mechanism with an indirect field-oriented induction servomotor drive directly. First, the mechanical structure and dynamic analyses of an elevator-door servomechanism was introduced. Moreover, the theoretical bases and stability analyses of the proposed TSMC systems were described in detail. In addition, simulation and experimentation were carried out using a specific reference profile to verify the effectiveness of the proposed control strategy. Compared with the CTC and CSMC systems, the TSMC system results in reduced chattering with robust control performance. The major contributions of this study are the successful development of a TSMC system, which has a total sliding motion without a reaching phase, and the successful application of the proposed TSMC system to control the motion of the elevator-door servomechanism considering the existence of uncertainties.

Acknowledgments

The authors would like to acknowledge the financial support of the National Science Council of Taiwan, R.O.C. through grant number NSC 90-2213-E-155-003. Moreover, the authors would like to thank Chuan Yao Machinery Co., Ltd. for the experimental setup and test facilities.

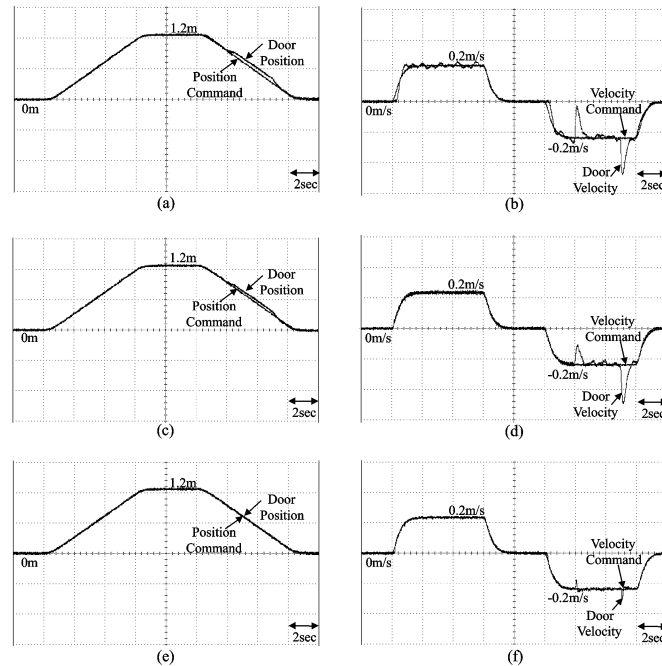


Figure 4.5. Experimental results of CTC, CSMC, TSMC systems at perturbed condition: (a) position tracking of CTC system; (b) velocity response of CTC system; (c) position tracking of CSMC system; (d) velocity response of CSMC system; (e) position tracking of TSMC system; (f) velocity response of TSMC system.

References

- [1] Lewis, F.L., Abdallah, C.T. and Dawson, D.M. *Control of Robot Manipulators*. Macmillan, New York, 1993.
- [2] Slotine, J.J.E. and Li, W. *Applied Nonlinear Control*. Prentice-Hall, New Jersey, 1991.
- [3] Astrom, K.J. and Wittenmark, B. *Adaptive Control*. Addison-Wesley, New York, 1995.
- [4] Khalil, H.K. *Nonlinear System*. Prentice-Hall, New Jersey, 1996.
- [5] Harashima, F., Hashimoto, H. and Kondo, S. MOSFET converter-fed position servo system with sliding mode control. *IEEE Trans. Ind. Electron.* **32**(3) (1985) 238–244.
- [6] Hashimoto, H., Yamamoto, H., Yanagisawa, S. and Harashima, F. Brushless servo motor control using variable structure approach. *IEEE Trans. Ind. Appl.* **24**(1) (1988) 160–170.
- [7] Gao, W. and Hung, J.C. Variable structure control for nonlinear systems: A new approach. *IEEE Trans. Ind. Electron.* **40**(1) (1993) 45–55.
- [8] Wai, R.J. Adaptive sliding-mode control for induction servomotor drive. *IEE Proc. Electr. Power Appl.* **147**(6) (2000) 553–562.
- [9] Leonhard, W. *Control of Electrical Drives*. Springer-Verlag, Berlin, 1996.
- [10] Krishnan, R. *Electric Motor Drives: Modeling, Analysis, and Control*. Prentice-Hall, New Jersey, 2001.
- [11] Kang, J.K. and Sul, S.K. Vertical-vibration control of elevator using estimated car acceleration feedback compensation. *IEEE Trans. Ind. Electron.* **47**(1) (2000) 91–99.
- [12] Pasanen, J., Jahkonen, P., Ovaska, S.J., Vainio, O. and Tenhunen, H. An integrated digital motion control unit. *IEEE Trans. Instrumentation and Measurement* **40**(3) (1991) 654–657.

- [13] Chung, D.W., Ryu, H.M., Lee, Y.M., Kang, L.W., Sul, S.K., Kang, S.J., Song, J.H., Yoon, J.S., Lee, K.H. and Suh, J.H. Drive systems for high-speed gearless elevators. *IEEE Industry Applications Magazine*, Sept./Oct. 2001, P. 52–56.
- [14] Hung, J.Y., Gao, W. and Hung, J.C. Variable structure control: A survey. *IEEE Trans. Ind. Electron.* **40**(1) (1993) 2–22.
- [15] Wai, R.J. Total sliding-mode controller for PM synchronous servo motor drive using recurrent fuzzy neural network. *IEEE Trans. Ind. Electron.* **48**(5) (2001) 926–944.